Comparison of YAG:Er and $YAlO_3$:Er laser crystals emitting near 2.9 μm

S. Wüthrich, W. Lüthy, and H. P. Weber
Institute of Applied Physics, University of Bern, Sidlerstrasse 5, CH-3012 Bern, Switzerland

(Received 26 April 1990; accepted for publication 2 August 1990)

Four different erbium laser crystals, two YAG:Er (40 at. %) and two $YAlO_3$:Er (30 at. % and 50 at. %), have been compared with respect to their laser thresholds and slope efficiencies. The performance of these laser crystals was further compared with a YSGG:Cr:Er ($Y_3Sc_2Ga_3O_{12}$) (3.6 at. % Cr^{3+} and 4 at. % Er^{3+}). The experimental results are explained with up-conversion processes in the crystals.

I. INTRODUCTION

Erbium lasers emitting near 2.9 μm are investigated mainly because of their potential applications in laser surgery. Familiar host crystals are YAG ($Y_3Al_5O_{12}$), $YAlO_3$, YLF ($LiYF_4$), or more recently GSGG ($Gd_3Sc_2Ga_3O_{12}$) or YSGG ($Y_3Sc_2Ga_3O_{12}$).[1] The performances of the different laser crystals were described in the literature.[1–8] They cannot, however, be compared directly with each other due to large differences in the efficiency of the individual pumping arrangements that were used. For this reason we have compared with respect to their thresholds and their slope efficiencies four different erbium doped laser rods operated in identical laser arrangements. In the present paper we report our experimental results and explain them with crystal internal processes.

For our investigations we had at disposal two YAG:Er rods with 40 at. % Er^{3+} concentration, one $YAlO_3$:Er with 30 at. % and one $YAlO_3$:Er with 50 at. % Er^{3+}. In addition we included a YSGG:Cr:Er with 3.6 at. % Cr^{3+} and 4 at. % Er^{3+} in our measurements. The properties of the investigated laser crystals are summarized in Table I.

II. EXPERIMENTAL SETUP

The laser rods were pumped with a pair of linear xenon flashlamps (ILC Model L4232) in a water-cooled diffusely reflecting pump cavity. To prevent the generation of color centers in the crystals, $NaNO_2$ (0.2 molar) was added to the coolant water to absorb pump radiation at wavelengths below 400 nm. Pump energies from threshold up to 92 J were used at a constant repetition rate of 4 Hz. The pulse duration was about 200 μs. The pump energy was varied by adjusting the flashlamp voltage. The 40-cm long laser resonator consisted of a flat mirror of 99.8% reflectivity and flat outcoupling mirrors with various reflectivities. Diffraction losses which normally have to be expected in resonators with flat mirrors were avoided due to the thermal lensing of the laser crystal.[4] The shape of the laser pulses was monitored with an InAs photodiode and a storage oscilloscope, the output energy with a pyroelectrical energy meter (Laser Precision RJ 7100). The pumplight was blocked with an edge filter (Corion RL-2000-F). Monomode emission was achieved with an aperture of 2.5 mm diam placed near the outcoupling mirror. The threshold and the output power were measured with various mirror reflectivities for each crystal. Other parameters, such as $NaNO_2$ concentration, resonator configuration, laser cavity, repetition rate, flashlamps, and load capacitance remained unchanged.

III. THEORY

In erbium doped crystals the erbium ion has an energy scheme with numerous states lying almost equidistant. Depending on the host crystal these states have slightly but influential different energy levels. We can therefore not predict the laser properties from the energy pumped into the upper laser states without considering for the respective crystals internal processes which either compete with or support the lasing process. In Table II, pairs of energy levels are tabulated that have similar energy differences as the $^4I_{13/2} \rightarrow {}^4I_{15/2}$ transition and hence may lead to resonant near-field pair interactions. From these processes only those are relevant for lasing that start from a highly populated level with a lifetime τ that is comparable to the duration of the excitation flashlamp pulse ($\tau \sim 100$ μs). Due to the UV absorbing coolant, starting levels higher than 25 000 cm^{-1} are not populated. The three most important processes are shown in Fig. 1. The 2.9-μm lasing transition takes place between the $^4I_{11/2}$ and $^4I_{13/2}$ state, the transition between the $^4I_{9/2}$ and the $^4I_{11/2}$ state is a fast ($\tau \sim 1$ μs) radiationless multiphonon transition.[9] A very important process labeled W_3 in Fig. 1 is the energy exchange between neighboring ions in the $^4I_{13/2}$ state with the reaction $^4I_{13/2} \rightarrow {}^4I_{15/2}$ and simultaneously $^4I_{13/2} \rightarrow {}^4I_{9/2}$ resulting in a depopulation of the lower laser state $^4I_{13/2}$ and a population of the upper $^4I_{11/2}$ laser level via the rapid $^4I_{9/2} \rightarrow {}^4I_{11/2}$ multiphonon transition. This up-conversion therefore supports in a twofold manner the population inversion essential for the lasing process. The probability rate

TABLE I. Properties of the investigated laser crystals with the pumped length L_p, the diameter in mm and the emission cross section σ in cm^2. The given reference refers to the cross section σ.

Crystal	Dopant conc.	L_p	Diam.	σ	Ref.
YAG:Er No. 1	40 at. %	55	6.35	2.6×10^{-20}	8
YAG:Er No. 2	40 at. %	55	6.35	2.6×10^{-20}	8
$YAlO_3$:Er	30 at. %	55	5.25		
$YAlO_3$:Er	50 at. %	55	4.90		
YSGG:Cr:Er	3.6 at. % Cr 4.0 at. % Er	61	4.30		

 0021-8979/90/235467-05$02.40

TABLE II. Possible cross-relaxation and up-conversion processes leading to a relaxation of the lower laser level to ground state Er^{3+} ($^4I_{13/2} \rightarrow {}^4I_{15/2}$). The data are for $YAlO_3$:Er. E_{start} gives the highest level from the manifold of the starting level as taken from Ref. 1. ΔE gives the spectral overlap between the manifolds of the indicated transition and $^4I_{13/2} \rightarrow {}^4I_{15/2}$. It is a qualitative value for the resonance condition. The given reference refers to the fluorescence lifetime τ of the starting level.

Transition	Er^{3+} Conc. at. %	τ (μs)	E_{start} (cm^{-1})	ΔE (nm)	Ref.
$^4S_{3/2} \rightarrow {}^2H_{9/2}$	15	1	18 487	70	13
$^4I_{9/2} \rightarrow {}^2H_{11/2}$	1	1	12 732	110	9
$^4G_{11/2} \rightarrow {}^2K_{13/2}$			26 526	145	
$^4I_{13/2} \rightarrow {}^4I_{9/2}$	15	4000	6868	12	13
$^4F_{9/2} \rightarrow {}^4F_{5/2}$	15	8	15 481	33	13
$^4F_{7/2} \rightarrow {}^4G_{9/2}$			20 685	44	
$^4F_{7/2} \rightarrow {}^2K_{15/2}$			20 685	33	
$^2H_{9/2} \rightarrow {}^2P_{3/2}$	1.25	800	24 765	40	14
$^4G_{9/2} \rightarrow {}^4G_{7/2}$			27 670	130	
$^2K_{15/2} \rightarrow {}^4G_{7/2}$			28 065	148	
$^2G_{7/2} \rightarrow {}^4G_{7/2}$			28 077	82	
$^4I_{9/2} \rightarrow {}^4S_{3/2}$	1	1	12 732	2	9

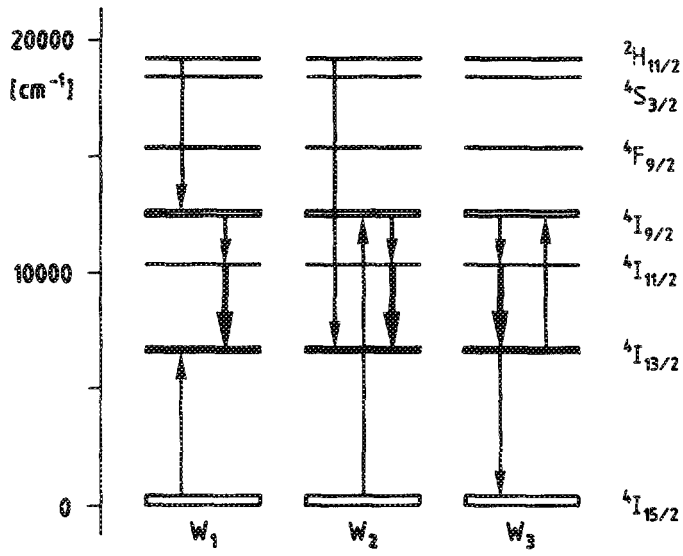

FIG. 1. Possible cross-relaxation (W_1 and W_2) and up-conversion (W_3) processes involving the $^4I_{13/2} \rightarrow {}^4I_{15/2}$ lasing transition.

for the process is proportional to the up-conversion coefficient W_3 and depends quadratically on the population n_2 in the $^4I_{13/2}$ state. Therefore highly doped crystals are necessary for efficient 3 μm laser operation. In YAG:Er the up-conversion coefficient has been determined.[10,11] Its value is about 2.5×10^{-17} $cm^3\,s^{-1}$ for 15 at. % erbium concentration. For $YAlO_3$:Er with 10 at. % erbium concentration the up-conversion coefficient is with 7.5×10^{-18} $cm^3\,s^{-1}$ (Ref. 12) more than three times smaller than in YAG:Er. It can be assumed that the coefficient depends on the spectral overlap of $^4I_{13/2} \rightarrow {}^4I_{15/2}$ and $^4I_{13/2} \rightarrow {}^4I_{9/2}$ transitions. In Table II also the spectral overlap between the manifolds of the involved transitions is given. This overlap is a qualitative measure for the resonance condition and the probability of these processes. Figure 2 shows the calculated positions of the lines in the $^4I_{13/2} \rightarrow {}^4I_{15/2}$ Stark sublevel manifold compared with the $^4I_{13/2} \rightarrow {}^4I_{9/2}$ manifold for YAG:Er and $YAlO_3$:Er. The spectral data are taken from Ref. 1. From the figure it can be seen that the range of spectral overlap (marked by arrows) in the case of YAG:Er is much larger than for $YAlO_3$:Er and that there are also more coincidences. The up-conversion process therefore is more probable in the YAG:Er crystal than in $YAlO_3$:Er. The other processes shown in Fig. 1, the cross-correlation processes W_1 ($^2H_{11/2} \rightarrow {}^4I_{9/2}$ with $^4I_{15/2} \rightarrow {}^4I_{13/2}$) and W_2 ($^2H_{11/2} \rightarrow {}^4I_{13/2}$ with $^4I_{15/2} \rightarrow {}^4I_{9/2}$) have nearly identical spectral overlaps. They populate the upper as well as the lower laser state. Due to the lifetimes of the different states they contribute to the population inversion but their probability is similar for YAG:Er and for $YAlO_3$:Er and they are therefore not thought to be responsible for the differences in efficiency.

IV. EXPERIMENTAL RESULTS

For the various crystals the dependencies of laser output vs input were measured in the described laser arrangement. The results for multimode emission are shown in Figs. 3(a)–3(e). Thresholds and slope efficiencies η_{mm} for multimode emission are summarized in Table III.

The lowest threshold of 17 J with a 92.5% mirror was measured with the YSGG:Cr:Er crystal. Since the pump energy was limited to 92 J, the threshold was not reached in YAG:Er and $YAlO_3$:Er crystals with the 50% and the 65% outcoupling mirrors. The highest output of 400 mJ was measured with the YAG:Er No. 2 crystal and a 92.5%

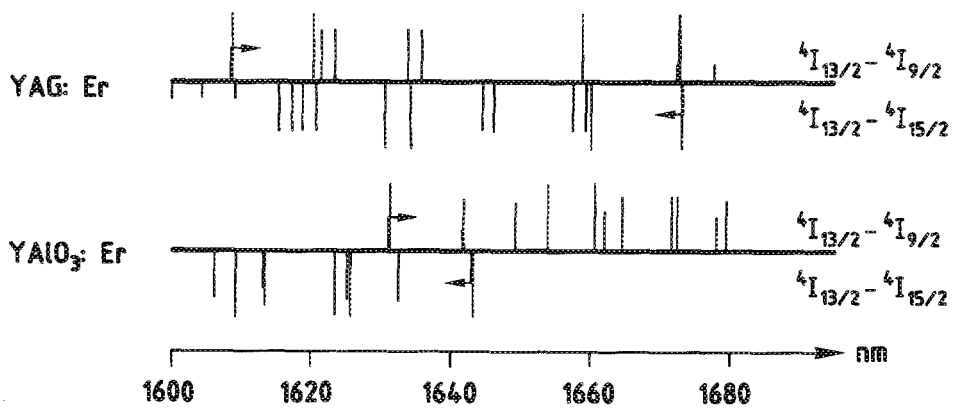

FIG. 2. Calculated values of the lines in the $^4I_{13/2} \rightarrow {}^4I_{9/2}$ manifold compared with the $^4I_{13/2} \rightarrow {}^4I_{15/2}$ manifold for YAG:Er and $YAlO_3$:Er. The length of each line is proportional to the probability of the transition according to the population of the respective Stark sublevel. In favor of a clear arrangement, transitions are plotted as lines instead of distributions.

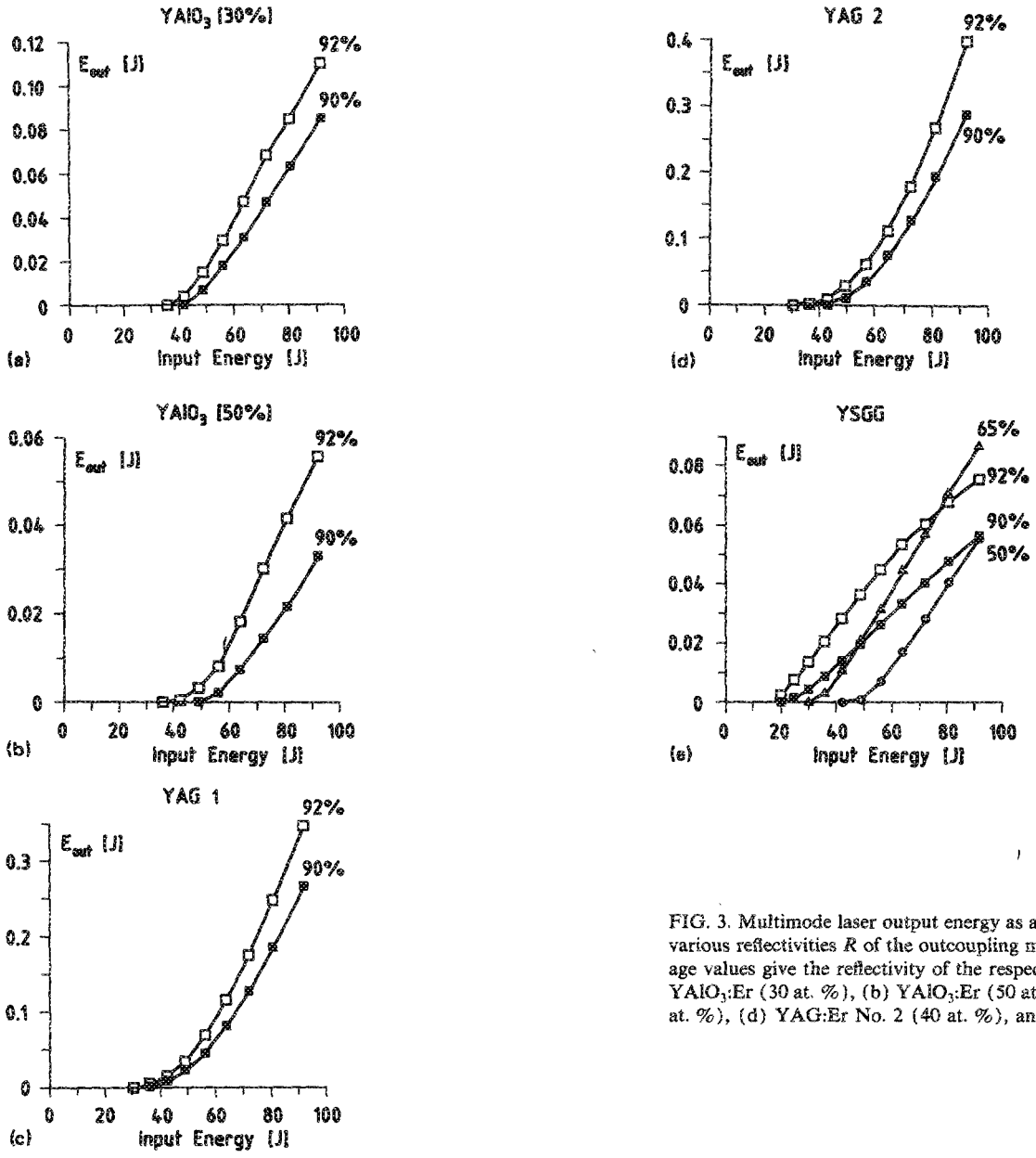

FIG. 3. Multimode laser output energy as a function of pump energy for various reflectivities R of the outcoupling mirror. The indicated percentage values give the reflectivity of the respective outcoupling mirror. (a) $YAlO_3$:Er (30 at. %), (b) $YAlO_3$:Er (50 at. %), (c) YAG:Er No. 1 (40 at. %), (d) YAG:Er No. 2 (40 at. %), and (e) YSGG:Cr:Er.

outcoupling mirror. Whereas for YAG:Er No. 1 and YAG:Er No. 2 the results correspond within 20%, the output energy of $YAlO_3$:Er (30 at. %) is four times lower. Values comparable with $YAlO_3$:Er (30 at. %) can be reached with YSGG:Cr:Er whereas $YAlO_3$:Er (50 at. %) is clearly inferior. With the exception of YSGG:Cr:Er that delivers highest output with a 65% outcoupling mirror, the other crystals showed best performance with the 92.5% outcoupling mirror. The highest slope efficiency of 1.1% was reached with the YAG:Er No. 2 crystal. The lowest threshold we measured for all crystals with the 92.5% outcoupling mirror.

TABLE III. Threshold energies E_{th} (J) and slope efficiencies η_{mm} (%) for the measured laser crystals and various reflectivities of the outcoupling mirrors for multimode operation.

	Outcoupling mirrors			
Crystals	50%	65%	90%	92.5%
$YAlO_3$:Er 30% E_{th}			42	38
$YAlO_3$:Er 30% η_{mm}			0.19	0.24
$YAlO_3$:Er 50% E_{th}			51	49
$YAlO_3$:Er 50% η_{mm}			0.09	0.13
YAG:Er No. 1 E_{th}			38	36
YAG:Er No. 1 η_{mm}			0.68	0.86
YAG:Er No. 2 E_{th}			40	38
YAG:Er No. 2 η_{mm}			0.80	1.10
YSGG:Cr:Er E_{th}	46	32	21	17
YSGG:Cr:Er η_{mm}	0.14	0.16	0.08	0.12

The results of the measurements performed with single transverse mode emission are given in Figs. 4(a)–4(d) and Table IV. Again, the lowest threshold resulted from the YSGG:Cr:Er crystal operated with a 92.5% mirror. In this configuration the highest output of 53 mJ was measured. The YAG:Er crystals reached nearly the same value. The highest value of the slope of single-mode efficiency η_{sm} was with 0.17% still reached with the YAG:Er No. 2 crystal, although the ratio η_{sm}/η_{mm} was clearly worse in the case of the YAG:Er crystals. For the YSGG:Cr:Er crystal we measured single-mode slope efficiencies η_{sm} similar to the

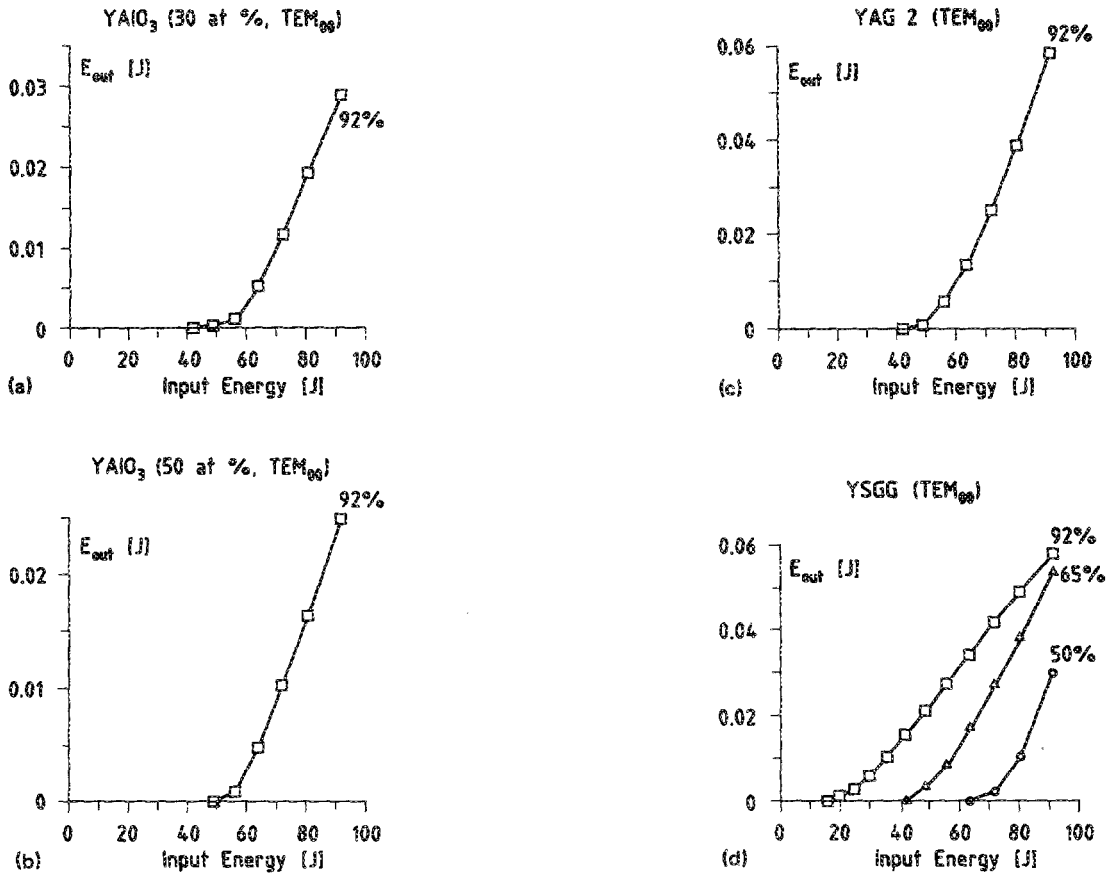

FIG. 4. Monomode laser output energy as a function of pump energy for various reflectivities R of the outcoupling mirror. The indicated percentage values give the reflectivity of the respective outcoupling mirror. (a) $YAlO_3$:Er (30 at. %), (b) $YAlO_3$:Er (50 at. %), (c) YAG:Er No. 2 (40 at. %), and (d) YSGG:Cr:Er.

values of η_{mm}. The reason for the various ratios between η_{mm} and η_{sm} lies in the different size of the crystals. Unfortunately, laser crystals with identical geometrical dimensions were not available. For multimode emission, the modifications introduced by this lack are however smaller than the significant differences of the multimode slope efficiency η_{mm}. In the case of single-mode emission, the differences in the rod diameters have to be taken into account. The reduction of the single-mode slope efficiency η_{sm} with respect to η_{mm} can partly be explained by the ratio between the small single-mode volume V_{sm} and the pumped volume V_p of the crystal. Values of η_{mm}/η_{sm} and V_p/V_{sm} are also given in Table IV. From Table IV it can be seen that the ratio η_{mm}/η_{sm} is correlated with the ratio V_p/V_{sm}.

TABLE IV. Threshold energies E_{th} (J) and slope efficiencies η_{sm} (%) for the measured laser crystals and various reflectivities of the outcoupling mirrors for single-mode operation. η_{mm}/η_{sm} gives the ratio of slope efficiencies in multimode operation η_{mm} to that of single-mode operation η_{sm}. These values are correlated with the ratio of pumped volume V_p to mode volume V_{sm}.

	Outcoupling mirrors			η_{mm}	V_p
Crystals	50%	65%	92.5%	η_{sm}	V_{sm}
$YAlO_3$:Er 30% E_{th}			53		
$YAlO_3$:Er 30% η_{sm}			0.08	3	4.4
$YAlO_3$:Er 50% E_{th}			56		
$YAlO_3$:Er 50% η_{sm}			0.07	1.9	3.8
YAG:Er No. 2 E_{th}			49		
YAG:Er No. 2 η_{sm}			0.17	6.5	6.5
YSGG:Cr:Er E_{th}	72	49	20		
YSGG:Cr:Er η_{sm}	0.15	0.13	0.09	1.3	3.0

For $YAlO_3$:Er η_{mm} or η_{sm} are 4–12 times lower than for YAG:Er. We make the radiationless energy transfer processes between the Er^{3+} ions responsible for such a large reduction.

The measured threshold energies are comparable for YAG:Er and $YAlO_3$:Er. The lowest value of 17 J however, has been measured with YSGG:Cr:Er. Due to codoping with chromium this threshold is lower by a factor of two with respect to YAG:Er or $YAlO_3$:Er. Cr^{3+} has broad absorption bands in the blue-green wavelength region well matched with the spectrum of the flashlamp. The efficient absorption of pumplight together with an energy transfer from Cr^{3+} to Er^{3+} results in a low threshold and high gain. In addition the high gain allows to use the YSGG:Cr:Er in Q-switch mode. The low efficiency of YSGG:Cr:Er on the other hand can be explained by its low dopant concentration.

V. CONCLUSION

We have compared four different erbium crystals—two YAG:Er (40 at. %) and two $YAlO_3$:Er (30 and 50 at. %)—with respect to their laser threshold and slope efficiency. The performance of these laser crystals was further compared with a YSGG:Cr:Er (3.6 at. % Cr^{3+} and 4 at. % Er^{3+}). The highest slope efficiency was found in YAG:Er, whereas the values for $YAlO_3$:Er and YSGG:Cr:Er were about three times lower. The difference in efficiency between YAG:Er and $YAlO_3$:Er is assigned to a lower up-conversion coefficient in the $YAlO_3$:Er due to the smaller spectral overlap of the resonances. The low efficiency of YSGG:Cr:Er can be explained by its low dopant concentration. The lowest threshold was measured with YSGG:Cr:Er due to co-doping with chromium which leads to an efficient absorption and subsequent transfer of pumplight to the erbium.

ACKNOWLEDGMENTS

We thank M. Frey and P. Herren for their stimulating interest and support. We also thank S. Schnell for helpful discussions and H. J. Weder for technical assistance. This work was supported in part by the Swiss Commission for the Encouragement of Scientific Research.

[1] A. A. Kaminskii, *Laser Crystals: Their Physics and Properties,* translation edited by H. F. Ivey (Springer, New York, 1981).

[2] S. Schnell, M. Stalder, and W. Lüthy, J. Phys. (Paris) Colloque, Suppl. **48**, C7–371 (1987).

[3] J. Frauchiger, W. Lüthy, P. Albers, and H. P. Weber, Opt. Lett. **13**, 964 (1988).

[4] J. Frauchiger and W. Lüthy, Opt. Laser Technol. **19**, 312 (1987).

[5] A. A. Kaminskii, T. I. Butaeva, A. O. Ivanov, I. V. Mochalov, A. G. Petrosyan, G. I. Rogov, and V. A. Fedorov, Sov. Tech. Phys. Lett. **2**, 308 (1976).

[6] E. V. Zharikov, V. I. Zhekov, L. A. Kulevskii, T. M. Murina, V. V. Osiko, A. M. Prokhorov, A. D. Savel'ev, V. V. Smirnov, B. P. Starikov, and M. I. Timoshechkin, Sov. J. Quantum. Electron. **4**, 1039 (1975).

[7] E. V. Zharikov, N. N. Il'ichev, S. P. Kalitin, V. V. Laptev, A. A. Malyutin, V. V. Osiko, P. P. Pashinin, A. M. Prokhorov, Z. S. Saidov, V. A. Smirnov, A. F. Umyskov, and A. Shcherbakov, Sov. J. Quantum Electron. **16**, 635 (1986).

[8] A. M. Prokhorov, in *Laser Spectroscopy VI,* edited by H. P. Weber and W. Lüthy (Springer, Heidelberg, 1983), pp. 427–429.

[9] A. A. Kaminskii, Sov. Phys. Dokl. **27**, 1039 (1982).

[10] V. I. Zhekov, V. A. Lobachev, T. M. Murina, and A. M. Prokhorov, Sov. J. Quantum Electron. **14**, 128 (1984).

[11] V. I. Zhekov, T. M. Murina, A. M. Prokhorov, M. I. Studenikin, S. Georgescu, V. Lupei, and I. Ursu, Sov. J. Quantum Electron. **16**, 274 (1986).

[12] M. A. Andriazian, S. M. Arutumian, R. B. Kostanian, and T. V. Sanamian, Press of the Academy of Science ASSR, Preprint Internal Report IFI-87-124 (1987).

[13] S. M. Arutyunyan, R. B. Kostanyan, A. G. Petrosyan, and T. V. Sanamyan, Sov. J. Quantum Electron. **17**, 1010 (1987).

[14] S. Schnell, P.-D. Henchoz, and W. Lüthy, J. Appl. Math. Phys. **39**, 918 (1988).